

UAV Icing: Experimental Investigation of Ice Shedding Times with an Electrothermal De-Icing System

Joachim Wallisch¹ and Richard Hann²

Norwegian University of Science and Technology, Trondheim, Norway
UBIQ Aerospace, Trondheim, Norway

Icing encounters can reduce the aerodynamic performance of aircraft significantly. To protect aircraft against the adverse effects of icing, ice protection systems are required. As of today, no mature ice protection systems exist for medium-sized fixed-wing unmanned aerial vehicles (UAVs). An important factor for the development of a de-icing system is to determine the required heat loads and heating periods. This work presents ice shedding times from experimental tests in an icing wind tunnel. An RG-15 airfoil equipped with a de-icing system is tested under conditions that are typical for medium-sized drones and cover the three icing regimes of glaze, mixed, and rime ice. The experiments show that increasing the ice protection system's heat flux reduces the time required for the ice to shed. However, the energy efficiency of the de-icing system decreases for higher heat fluxes. Another finding is that the angle of attack influences the shedding times significantly. While the effect of intercycle times on the shedding time depends on the temperature, the system becomes more energy-efficient for longer intercycle times for all temperatures. These results help to define more energy-efficient operation procedures for ice protection systems for UAVs.

I. Introduction

The market for unmanned aerial vehicles (UAVs), often also called unmanned aerial systems (UAS), remotely piloted aircraft systems (RPAS), or drones, is growing significantly because of the wide variety of missions they can operate [1]. However, the availability of UAVs is limited by extreme weather conditions. One particularly dangerous weather condition is icing [2]. Atmospheric icing, also known as in-flight icing or in-cloud icing, happens when aircraft fly through clouds containing supercooled droplets. The droplets will freeze on the surfaces they hit and cause performance degradation. Ice on the wings decreases the aerodynamic performance [3], ice on the propeller or at the engine decreases the thrust of the aircraft [4], and ice on sensors or antennas can make them behave faultily or stop working [5]. As previous accidents have shown, the negative effects of icing can be severe enough to cause aircraft to crash [5].

Ice protection systems (IPS) can reduce the negative impact of icing on aircraft performance [6]. Hence, equipping an aircraft with an IPS enables the aircraft to operate safely in icing conditions that the IPS was designed for. Mature IPS exist for manned aviation after research has been performed for decades [6]. But, because of the differences between manned and unmanned aircraft, IPS cannot be simply transferred from manned aircraft to UAVs [2]. Some of the key differences between manned aircraft and unmanned aircraft are related to weight, mission profiles, altitude, propulsion system, and autonomy [2]. The size and velocity of medium-sized fixed-wing UAVs pose a new challenge. The flight Reynolds numbers of those UAVs are typically two orders of magnitude smaller compared to manned aircraft. This difference in Reynolds number can lead to different flow regimes involved in the icing process [7,8]. As a result, more research on UAV icing is required. Because of the lack of an IPS, every operation of UAVs in icing

¹ PhD Student, Centre for Autonomous Marine Operations and Systems (AMOS), Department of Engineering Cybernetics, Norwegian University of Science and Technology (NTNU), E-mail: joachim.wallisch@ntnu.no.

² Researcher, Centre for Autonomous Marine Operations and Systems (AMOS), Department of Engineering Cybernetics, Norwegian University of Science and Technology (NTNU).

conditions carries the risk of losing the aircraft, and typically UAVs will not be deployed into known icing conditions [9].

While UAVs are already used widely, having them grounded during icing conditions blocks new UAV markets and UAV missions. Some missions require a high degree of availability, regardless of the meteorological conditions. Examples would be the transport of human organs for transplants or patrolling a border [10,11]. In both cases, having the UAV grounded for a significant time endangers the mission's success. To transition those missions to UAVs, good availability of the UAVs is required. A second possible UAV market that is blocked by having the aircraft grounded during icing conditions is consumer-related. Over the last years, the topics of drone parcel delivery and urban air mobility have received interest. While the availability of the aircraft is not safety-critical in this area, it is critical for the customers' decision to pay. If the operator would have to cancel the parcel delivery or the urban air mobility transport too often, customers would stick with traditional means because of the reliability. Hence, developing IPS for UAVs can open many new markets.

One particularly important aspect of an IPS for UAVs is energy efficiency. UAVs typically only carry a limited amount of energy on board. This energy will be used to power the propulsion system and the payload and would also be used to power the IPS. Hence, every IPS that requires energy reduces the endurance and the range of the aircraft. If the IPS is not energy-efficient, it might reduce the endurance and the range of the UAV below the requirements of the mission.

One example of an IPS for medium-sized fixed-wing UAVs is D-ICE. D-ICE is an electrothermal IPS that was originally developed at the Centre for Autonomous Marine Operations and Systems (AMOS) at the Norwegian University of Science and Technology (NTNU) and is now commercially developed by UBIQ Aerospace. The principle of thermal IPS is to heat the wing surface to either prevent the accretion of ice (anti-icing) or to periodically remove the ice (de-icing) [6]. A previous study on this system has shown that the operation of an electrothermal IPS is more energy-efficient in de-icing mode than in anti-icing mode [12]. Additionally, using an electrothermal IPS with a parting strip – a continuously heated element at the leading edge - is more energy-efficient than using a conventional configuration [12]. This is because the ice must not be completely melted when using a de-icing system with a parting strip. Instead, once a water layer with sufficient dimensions exists between the wing surface and the ice layer, the ice will shed because the aerodynamic forces are greater than the surface adhesion of the ice [13,14].

The objective of this study was to determine the required heat loads and heating periods of an IPS and to investigate the energy efficiency. Experimental tests were conducted in an icing wind tunnel. An RG-15 airfoil, equipped with a prototype of the electrothermal D-ICE system, was tested under typical operating conditions of a medium-sized UAV. The results show the de-icing times for different power settings of the IPS and several icing conditions. The ice shedding times are an important parameter for the performance of IPS and can provide information for further IPS designs. This new study is the continuation of previous work [12], but investigates new aspects to gain a deeper understanding: The new results have been obtained with a wing with a shorter chord length compared to previous tests. Hence, the new results are closer to actual medium-sized UAVs. Additionally, the angle of attack range tested was wider in the new study, providing information for more flight phases. During the experiments of the previous study, all zones have been operated with the same heat flux. The new study also tested operating different zones with different heat fluxes to potentially improve energy efficiency.

II. Methods

Experimental tests were performed in the icing wind tunnel of the Technical Research Centre of Finland (VTT) in Helsinki [15]. The open-loop wind tunnel is located inside a cold room. The temperature inside the cold room can be controlled between -20 and $+25$ °C. Wind speeds up to 50 m/s are possible inside the icing wind tunnel and enable testing at typical UAV airspeeds. A 3x3 spray bar injects liquid water droplets into the air stream. The liquid water content LWC can be controlled between 0.1 and 1.0 g/m³ and the median volume droplet diameter MVD between 17 and 35 μm .

Two different wings were used during the experiments. Most results were generated with a wing with constant chord length. The wing uses the RG-15 airfoil. Because the RG-15 was developed for low Reynolds numbers, it is a typical airfoil for medium-sized UAVs. The chord length of the tested wing is 0.3 m, and the span is 0.7 m. To increase the accessibility and the visibility of the wing during the experiments, the icing wind tunnel was operated in an open test section configuration. Since the rectangular wing spans almost the whole width of the icing wind tunnel test section, the results in this study are considered to be representative for the results of a 2D airfoil. One series of runs was performed with a swept wing. This wing also uses the RG-15 airfoil and has a mean aerodynamic chord length of 0.3 m. The swept test wing was derived from a real UAV wing with a larger span, but only the section closer to the fuselage was used for tests.

Both wings were made from glass fiber-reinforced plastic and were based on the D-ICE system. Figure 1 shows the IPS design that consists of a parting strip and four heating zones, two on the upper surface and two on the lower surface. A thin heating wire is used as the parting strip. It is located at the leading edge of the wing and integrated directly underneath the glass fiber-reinforced layer. The four heating zones are made from carbon fibers and integrated into the wing structure as explained in [12]. The primary heating zones, i.e., the carbon zones closer to the leading edge, are 20 mm long and the secondary heating zones have a chord-wise length of 60 mm. All heating zones cover the whole span of the wing. The carbon fibers are powered by an external power source and thus provide heat to de-ice the wing. The power supply to each zone is controlled individually with pulse-width modulation [16].

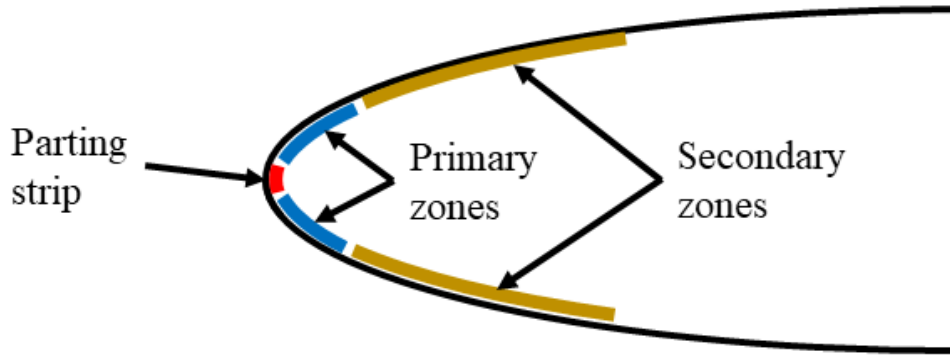


Fig. 1 The IPS of the wing consists of four heating zones and one parting strip.

The test conditions were chosen to replicate typical operating conditions for medium-sized fixed-wing UAVs. The airspeed was held at 25 m/s, yielding a Reynolds number of 6×10^5 . This is a typical flight Reynolds number for medium-sized fixed-wing UAVs [17]. Different angles of attack were tested to replicate different flight phases and to test the effect of the angle of attack on icing. In this study, tests were performed at -4° , 0° , 4° , 8° , and 12° angles of attack.

To reduce the calibration work, only one combination of *LWC* and *MVD* was tested. The *LWC* was held at 0.44 g/m^3 and the *MVD* was $24 \text{ }\mu\text{m}$. These values were chosen because they are quite common for in-cloud icing. Hence, the temperature was the only parameter that was adjusted to account for different icing conditions. Tests were performed at temperatures of -2°C , -5°C , -10°C , and -15°C . With this temperature range, the three different icing conditions – glaze, mixed, and rime [18] – can be covered. Table 1 summarizes the range of conditions that were used for tests.

The heat fluxes in heat zones on the pressure side were identical to the heat fluxes in the matching heat zones on the suction side. Unless noted specifically, all runs were conducted with the rectangular wing using the same heat flux in the primary and in the secondary zones, having 0° angle of attack, and running for four minutes.

The reason for using a parting strip is to keep the leading edge ice-free at all times. The required parting strip power depends especially on the ambient temperature and has been investigated in the past, e.g. [12]. For this study, it was only checked if the power from previous experiments could be used for the new experiments as well. To verify the parting strip power, an ice accretion run was done for 2 minutes while only the parting strip was powered and no other zone. The ice gap at the leading edge was checked optically after the run. If the ice gap was not approximately 0.5 mm, the power was changed accordingly, and a new test was performed. The final parting strip powers that were used in this study are shown in Table 2.

Table 1 The range of test conditions.

Parameter	Tested conditions
Airspeed	25 m/s
Temperature	-2°C ; -5°C ; -10°C ; -15°C
<i>LWC</i>	0.44 g/m^3
<i>MVD</i>	$24 \text{ }\mu\text{m}$
Angle of attack	-4° ; 0° ; 4° ; 8° ; 12°
Intercycle time	4 min, 6 min, 8 min

Table 2 The parting strip powers used for the tests.

Temperature	Parting strip power
-15°C	70 W
-10°C	45 W
-5°C	17 W
-2°C	8 W

After the parting strip power had been verified, de-icing runs were performed. All runs followed the same test sequence to increase the repeatability:

- First, the wind was started in the icing wind tunnel.
- Thirty or sixty seconds later, the spray nozzles in the icing wind tunnel were started as well. At the same time, the parting strip was started to have an ice gap at the leading edge during the whole run.
- After the time specified for the run – typically four minutes – the de-icing procedure was started. This means that heating of the primary and secondary heating zones was activated.
- The time between the start of the de-icing procedure and the first occasion of ice shedding was captured with a stopwatch and written down. Because the ice did not shed at all locations at the same time, the first occasion of ice shedding in the central part of the upper side of the wing was considered representative of the whole wing.
- After the ice had shed, the IPS, the spray nozzles, and the wind inside the icing wind tunnel were stopped.
- After the whole wing was cleaned from remaining ice and after all heating zones had cooled down to the ambient temperature, the next run was started.

To increase the comparability of different test runs, all runs followed exactly the procedure explained above. The test equipment was kept inside the cold room the entire time to reduce temperature influences on the results. Additionally, the same person operated the stopwatch for every run.

The experiments were also filmed using multiple cameras in the cold room. However, the video quality was typically bad. Additionally, the IPS had to be started manually and the videos did not contain a clear signal of the activation time of the IPS. Hence, it was not possible to detect the exact shedding times using the videos. However, it was possible to compare differences in ice shedding behaviors for different runs. These comparisons helped in analyzing and understanding the data.

The intention was to have multiple repetitions of each run to reduce the measurement uncertainty. However, due to time constraints, it was not possible to test each condition multiple times. To differentiate between conditions that were tested only once and conditions that were repeated, two different styles are used in this paper. Conditions that were only tested once are denoted with a single point in the following figures. For runs that were repeated at least once, the average is shown with a point in the figures, and error bars show the measurement uncertainty of the time measurement. The measurement uncertainty was calculated using Student's t-distribution [19]. During the calculation, random errors were considered as well as possible human errors. Human errors could occur during reading the stopwatch after detecting the shedding and because the IPS was started manually and no signal showed the start of the IPS in the cold room. To be conservative, the possible human errors were assumed to be 1.5 seconds. The error bars in the plots show a confidence interval of 90%. This confidence interval was considered accurate for showing important trends of the tests done in this study.

While ice shedding times are important knowledge for a de-icing system, a better measure of the quality of an IPS might be the energy efficiency. The time-averaged energy

$$\bar{q} = \frac{(q_{Primary} + q_{Secondary}) \cdot t_{Shedding} + q_{Parting\ strip} \cdot (t_{Intercycle} + t_{Shedding})}{t_{Intercycle} + t_{Shedding}} \quad (1)$$

was introduced as a measure of the energy efficiency of the de-icing sequence [12]. It takes the shedding time $t_{Shedding}$ into account as well as the power used for the IPS. $q_{Primary}$ and $q_{Secondary}$ denote the power supplied to both primary and secondary heating zones, respectively, and $q_{Parting\ strip}$ is the power used to heat the parting strip. The intercycle time $t_{Intercycle}$ denotes the time of the experimental runs in which only the parting strip was active. Runs with lower time-averaged energy are more energy-efficient.

III. Results

A. The influence of the heat flux

Several factors influence the ice shedding time. The first tests compare the shedding times for different temperatures and different heat fluxes. Tests were performed at $-2\text{ }^{\circ}\text{C}$ using heat fluxes of 4 kW/m^2 , 8 kW/m^2 , 12 kW/m^2 , and 18 kW/m^2 , and at $-5\text{ }^{\circ}\text{C}$ using heat fluxes of 8 kW/m^2 , 12 kW/m^2 , and 18 kW/m^2 .

As can be seen in Fig. 2, higher heat fluxes lead to faster ice shedding times independent of the ambient temperature. This is because higher heat fluxes result in higher temperatures at the different layers of the ice protection system and at the interface between the wing and the ice. Hence, the ice starts melting quicker when using higher heat fluxes, and thus, the ice sheds earlier when the heat flux is higher.

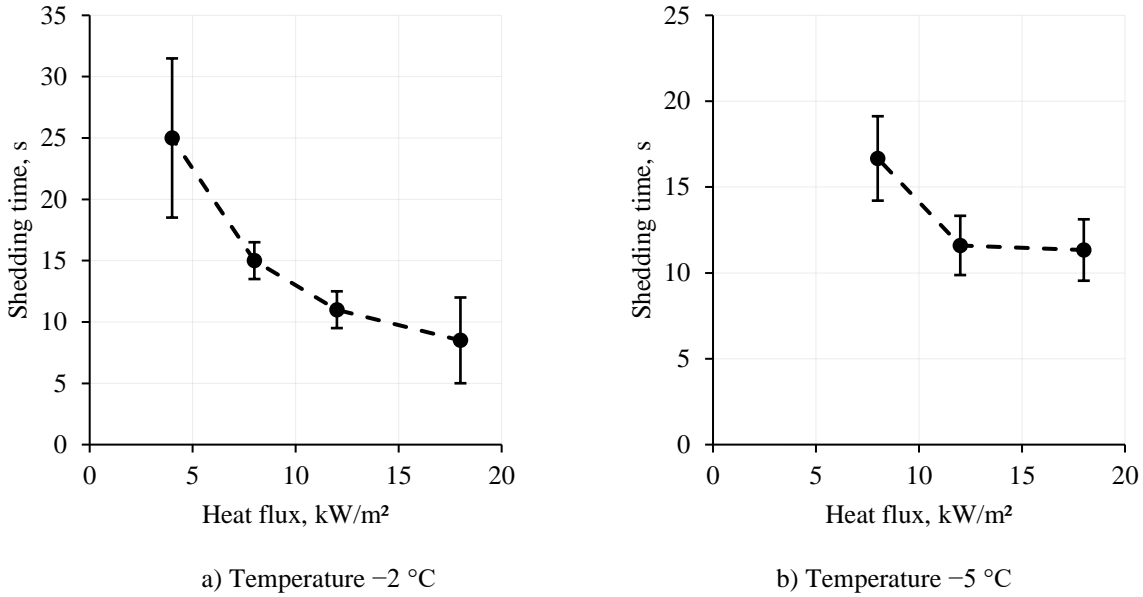


Fig. 2 The ice shedding times and measurement uncertainties for different heat fluxes at a) $-2\text{ }^{\circ}\text{C}$ and b) $-5\text{ }^{\circ}\text{C}$.

Faster shedding is not equivalent to more energy-efficient de-icing. On the contrary, when using Eq. (1), runs with lower heat fluxes require less time-averaged energy \bar{q} , see Fig. 3. One possible explanation is that using higher heat fluxes not only increases the surface temperature of the wing, but also the temperatures inside the wing. Hence, more energy is used to heat the inside of the wing for higher heat fluxes. This heat is not used directly to melt the ice and thus, reduces the energy efficiency of the de-icing sequence. Another possible explanation is that heat conduction takes some time. Powering the heating zones of the wing does not result in an immediate increase in temperature at the surface of the wing. Instead, the surface temperature of the wing only starts rising with a short delay. Hence, some heat generated in the heating zones has not been conducted to the surface of the wing when the ice sheds. This part of the heat could be larger for higher heat fluxes and would thus result in lower energy efficiency.

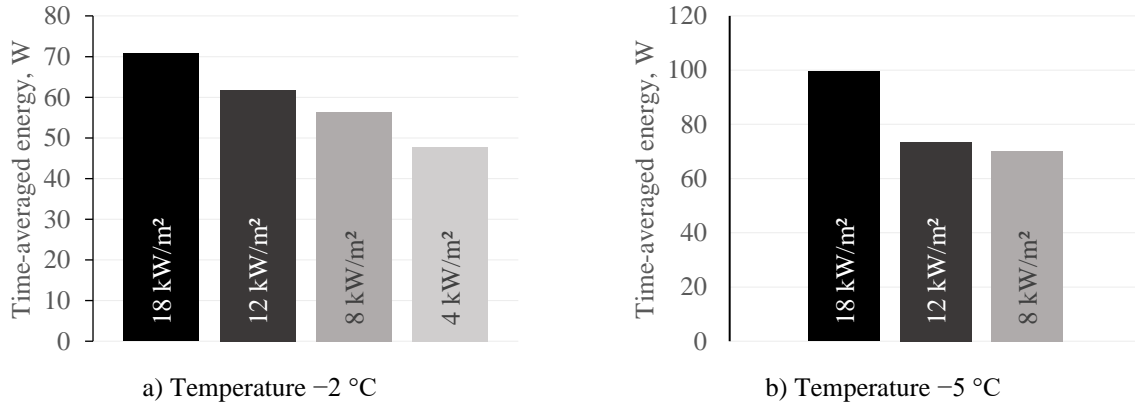
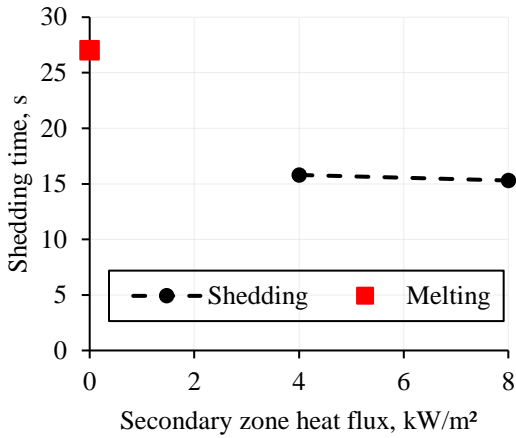


Fig. 3 The time-averaged energy requirements for de-icing with different heat fluxes at a) $-2\text{ }^{\circ}\text{C}$ and b) $-5\text{ }^{\circ}\text{C}$.

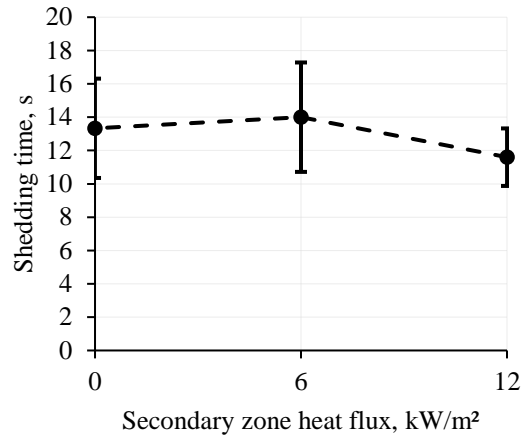
B. The influence of the heat flux in secondary zones

Typically, most ice accretes in the vicinity of the leading edge. To test the significance of the secondary zone heat flux on ice shedding, tests have been performed with fixed heat fluxes in the primary zones and different heat fluxes in the secondary zones. Tests have been performed at $-2\text{ }^{\circ}\text{C}$, $-5\text{ }^{\circ}\text{C}$, and $-15\text{ }^{\circ}\text{C}$. The heat flux in the primary zone was kept at 8 kW/m^2 for $-2\text{ }^{\circ}\text{C}$, at 12 kW/m^2 for $-5\text{ }^{\circ}\text{C}$, and at 18 kW/m^2 and 24 kW/m^2 for $-15\text{ }^{\circ}\text{C}$, respectively.

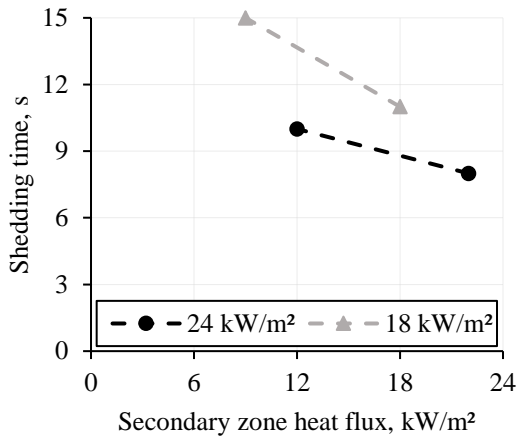
The results do not show a clear trend, see Fig. 4. At the warmer temperatures of $-2\text{ }^{\circ}\text{C}$ and $-5\text{ }^{\circ}\text{C}$, the shedding times appear almost constant for different secondary zone heat fluxes. At the colder temperature of $-15\text{ }^{\circ}\text{C}$, increasing



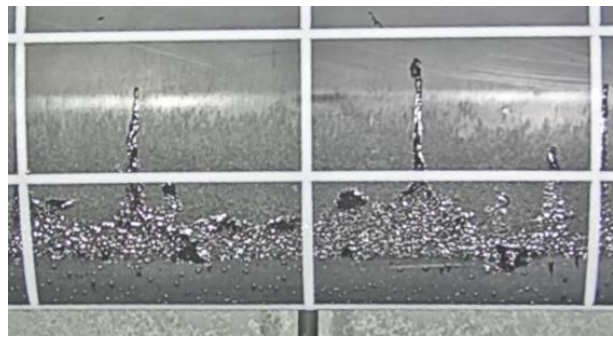
a) Temperature -2 °C



b) Temperature -5 °C



c) Temperature -15 °C



d) Remaining ice after a run without secondary zone heat flux

Fig. 4 The ice shedding times for different secondary zone heat fluxes at a) -2 °C, b) -5 °C, and c) -15 °C. When using no heat in the secondary zone at -2 °C, the ice did not shed but only melted. Part d) shows the ice that remains after de-icing when using no secondary zone heat at -5 °C.

the secondary zone heat flux accelerated the shedding. When using no heat flux in the secondary zone at -2 °C, the ice did not shed but only melted and it took much longer to remove the ice from the wing.

The video footage of the runs was checked closely to find possible explanations for the rather small and inconsistent influence of the secondary zone heat flux. Two distinct features could be seen in the videos. First, the amount of ice that sheds is different for different secondary zone heat fluxes. While the ice in the primary zone always sheds, the ice in the secondary zone depends on the heat flux. For high heat fluxes in the secondary zone, the shedding removes almost all of the accreted ice. Only a very thin layer of ice in the more downstream areas does not shed but will be blown off the wing as well. Reducing the heat in the secondary zones leads to a different shedding behavior. When the ice that is close to the leading edge sheds, the ice located further downstream remains on the wing. It appears that the ice breaks into two parts while the primary part sheds. If the secondary zone is slightly heated, the remaining ice will melt and slide off the wing due to the aerodynamic forces. If the secondary zone is not heated, the ice will remain there, as can be seen in Fig. 4 d).

A second distinct feature is that the ice often moves slightly downstream before it sheds. This could mean that the adhesive forces are too high to allow shedding at this moment but low enough to allow sliding. Another explanation for the sliding could be that the aerodynamic forces attack under an angle that does not lead to a leveraging effect of the ice. Within a second of sliding downstream, the ice or parts of the ice normally detach and shed.

For cases with reduced secondary zone heat flux at $-15\text{ }^{\circ}\text{C}$, a small strip of ice appeared solid after the other parts of the ice had started melting. The other runs did not show a part of ice that started melting significantly later than the rest. This strip of ice likely kept the ice from sliding and hence, delayed the shedding process. The location of the strip of ice was approximately at the transition from the primary to the secondary zone. This area is not heated and hence, ice can only melt there if enough heat is conducted from the two heating zones. The conducted heat was likely not enough to overcome the large temperature difference between ambient temperature and melting temperature for the two cases with low secondary zone heat flux at $-15\text{ }^{\circ}\text{C}$.

Additionally, the ice shape appears to play a role for the shedding times. The ice shapes at $-5\text{ }^{\circ}\text{C}$ seemed to have ice horns close to the stagnation point. Those ice horns would increase the aerodynamic forces significantly. This could explain why ice sheds at $-5\text{ }^{\circ}\text{C}$ when no secondary zone heat flux is used while the ice only melts at $-2\text{ }^{\circ}\text{C}$. At $-2\text{ }^{\circ}\text{C}$, the freezing fraction close to the leading edge is smaller and hence, less ice builds resulting in lower aerodynamic forces [12].

C. The influence of the angle of attack

An aircraft will typically not operate under a single fixed angle of attack, but the angle of attack will change during flight and depending on the flight operation. To test the effect that the angle of attack has on de-icing, the wing was tested at different angles of attack at $-5\text{ }^{\circ}\text{C}$ and $-10\text{ }^{\circ}\text{C}$. For these tests, the heat fluxes were chosen to be identical for primary and secondary heating zones. At $-5\text{ }^{\circ}\text{C}$, the heat flux was 12 kW/m^2 , and at $-10\text{ }^{\circ}\text{C}$, the heat fluxes were 12 kW/m^2 and 18 kW/m^2 , respectively.

The results at $-5\text{ }^{\circ}\text{C}$ show a trend of decreasing ice shedding times with increasing angles of attack, see Fig. 5 a). This is likely due to three effects. First, at higher angles of attack less ice accretes at the upper side of the wing. Second, an increase in angle of attack also increases the local speed at the upper side of the aircraft. This results in larger aerodynamic forces that work on the ice and lead to faster shedding. Third, as suggested by Hann, et. al. [12], the increase in local airspeed could also increase the convective heat transfer from the air warmed up by the parting strip. This would lead to faster melting of the ice accreted on the wing.

The measured ice shedding times at $-10\text{ }^{\circ}\text{C}$ have different behaviors for different heat fluxes as can be seen in Fig. 5 b). At the lower heat flux, the ice shedding times decrease with increasing angles of attack as for the warmer case. However, the higher heat flux shows a minimum in shedding time for 0 and 4 ° angle of attack and an increase in shedding times with decreasing and increasing angles of attack from this minimum. The increased shedding times for high angles of attack contrast with the other tests. After checking the video material from the tests, the outliers look like measurement errors, but due to suboptimal video quality, this can not be said for sure. However, one particular problem with the runs with high angles of attack is that only a very little amount of ice accretes. That makes it more difficult to see the shedding.

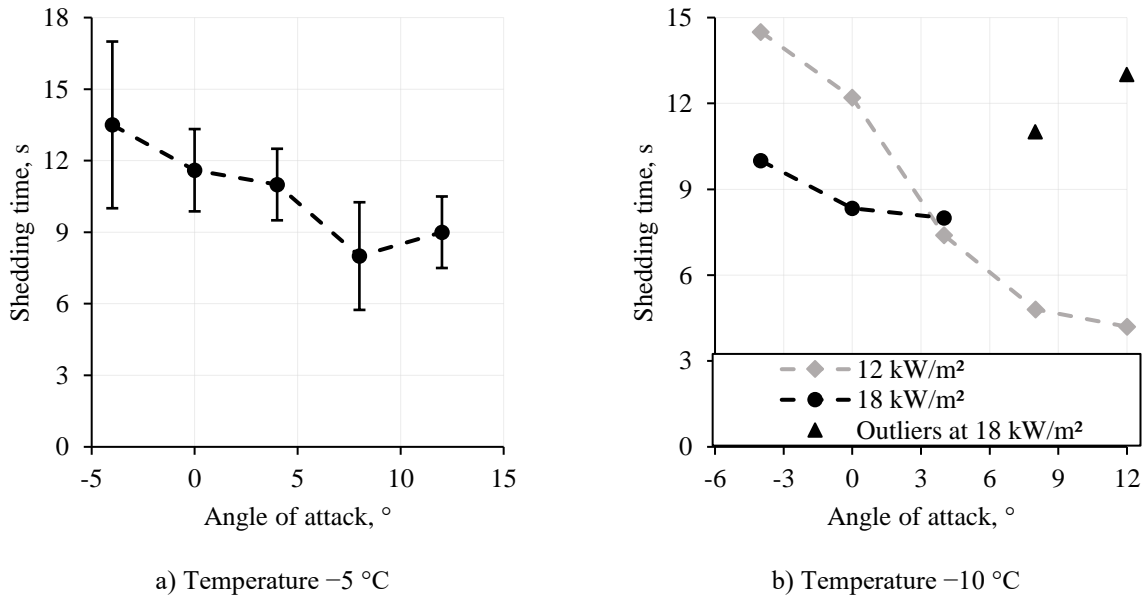


Fig. 5 The ice shedding times for different angles of attack at a) $-5\text{ }^{\circ}\text{C}$ and b) $-10\text{ }^{\circ}\text{C}$. Outliers are denoted with triangles and are likely due to incorrect measurements.

D. The influence of the intercycle time

An important variable for de-icing systems is the intercycle time. It describes the time between two de-icing cycles. Tests with different intercycle times were performed at two different temperatures, $-2\text{ }^{\circ}\text{C}$ and $-10\text{ }^{\circ}\text{C}$. All runs used the same heat fluxes in the primary and the secondary zones. At $-2\text{ }^{\circ}\text{C}$, 8 kW/m^2 , 12 kW/m^2 , and 18 kW/m^2 were used as heat fluxes. At $-10\text{ }^{\circ}\text{C}$, the heat flux was kept at 18 kW/m^2 .

While longer intercycle times accelerated the ice shedding for the warmer temperatures of $-2\text{ }^{\circ}\text{C}$, the shedding took longer for longer intercycle times at $-10\text{ }^{\circ}\text{C}$, see Fig. 6. This effect might be related to the different ice shapes for different temperatures. At glaze temperatures like $-2\text{ }^{\circ}\text{C}$, the ice shape normally has characteristic ice horns. Those horns grow bigger for longer intercycle times. This would increase the aerodynamic forces with longer intercycle times and accelerate the shedding. At rime temperatures like $-10\text{ }^{\circ}\text{C}$, the ice shape normally has no characteristic feature but acts rather like a thickening of the airfoil. An increase in thickness has a significantly lower effect on the aerodynamic forces, but more ice must be melted to have the same relative liquid layer thickness, resulting in slower shedding.

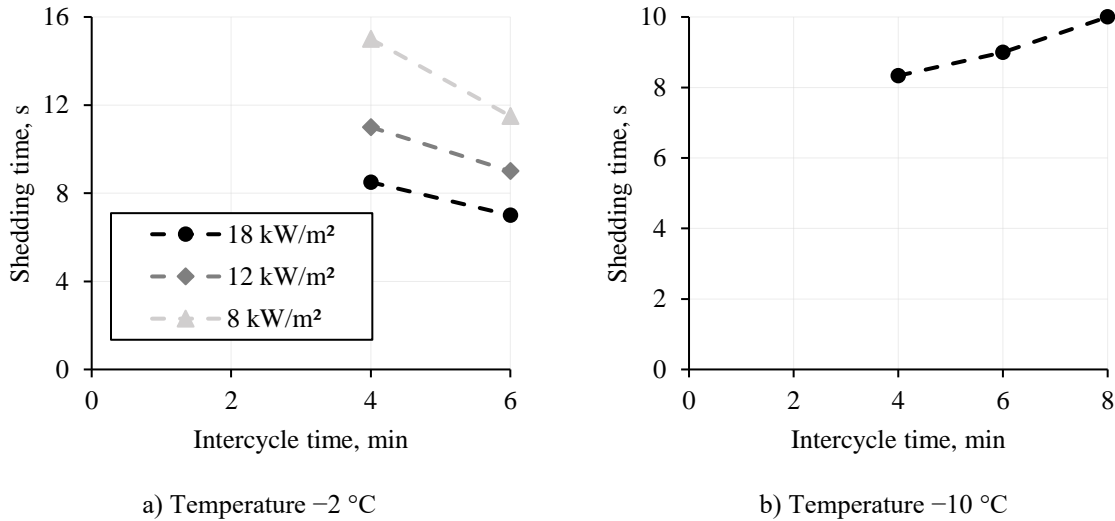


Fig. 6 The ice shedding times for different intercycle times at a) $-2\text{ }^{\circ}\text{C}$ and b) $-10\text{ }^{\circ}\text{C}$.

While the influence of different intercycle times on the ice shedding times appears to be temperature-dependent, the trend of the energy efficiency is clear. For all different temperatures and heat fluxes, longer intercycle times make the de-icing more energy-efficient, see Fig. 7. This is because by using the parting strip design, not all the accreted ice must be melted. Instead, only a liquid layer with sufficient thickness must be created between the wing surface and the ice layer [14].

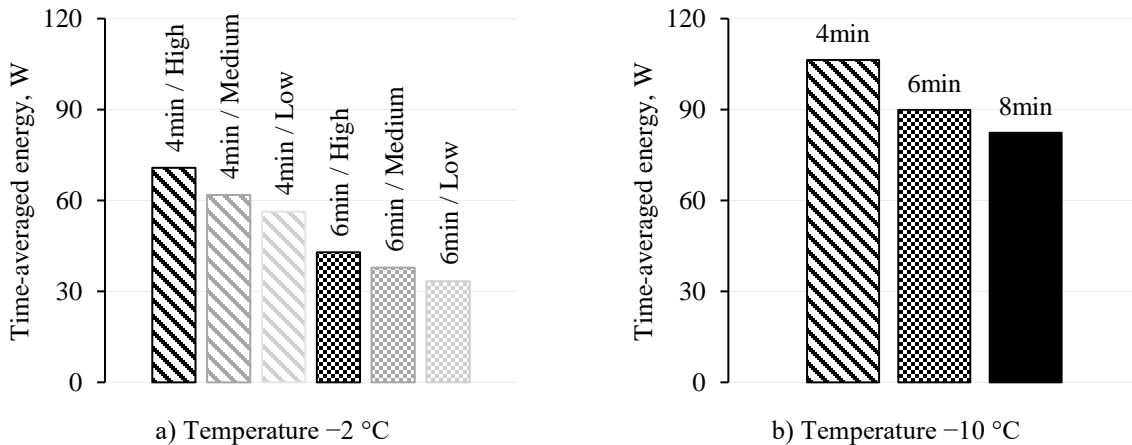


Fig. 7 The time-averaged energy for different intercycle times and different heat fluxes.

E. The influence of delayed parting strip activation

All previous results were obtained by starting the parting strip at the same time as the spray nozzles of the icing wind tunnel. In real flight, however, icing encounters are typically not recognized immediately. If the IPS is not active during the whole flight, it will typically be activated once icing conditions are identified. Depending on the quality of the ice detection sensors and on the icing conditions, the detection of icing conditions can take some seconds.

Tests were done to check for the effect that the delayed activation of the parting strip has on de-icing. A swept wing was used for those tests at $-2\text{ }^{\circ}\text{C}$. The heat flux was 8 kW/m^2 in the primary zones and 4 kW/m^2 in the secondary zones. To have a comparable amount of ice accreted on the wing, the de-icing was activated four minutes after starting the spray nozzles for all cases. Hence, if the parting strip was activated with a delay of 60 seconds, the time difference between the activation of the parting strip and the de-icing sequence was only three minutes.

The runs with delayed activation of the parting strip often had no clear shedding event, but rather showed a mixture of shedding, melting, and sliding. Hence, for the comparison of these runs, the time between the activation of the de-icing system and the complete removal of ice from the wing was measured. Delayed activations of the parting strip increase the time until the ice is removed from the wing significantly, see Fig. 8. This is because a layer of ice has accreted at the leading edge before the parting strip is activated. The parting strip must then melt the accreted ice while new droplets hit the wing and will freeze if the heat flux is not large enough. Because the parting strip power was selected for simultaneous activation with the icing cloud, the parting strip is not powerful enough to remove all the ice before the de-icing cycle starts. Hence, those runs are much more comparable to conventional de-icing runs, i.e., almost all the ice is melted and there is little to no ice shedding. This is also shown by the run with increased parting strip power that was de-iced faster than the runs with lower parting strip power.

An interesting finding of these experiments was also that a few seconds after starting the de-icing, the ice started to move laterally on the wing. This could be because the lowest layers of ice had melted and hence the adhesive forces were small. Due to the ice bridge that remained at the leading edge because of the delayed parting strip activation, the ice could not shed. Because of the lateral velocity at swept wings, the ice would then start to move towards the outside of the wing.

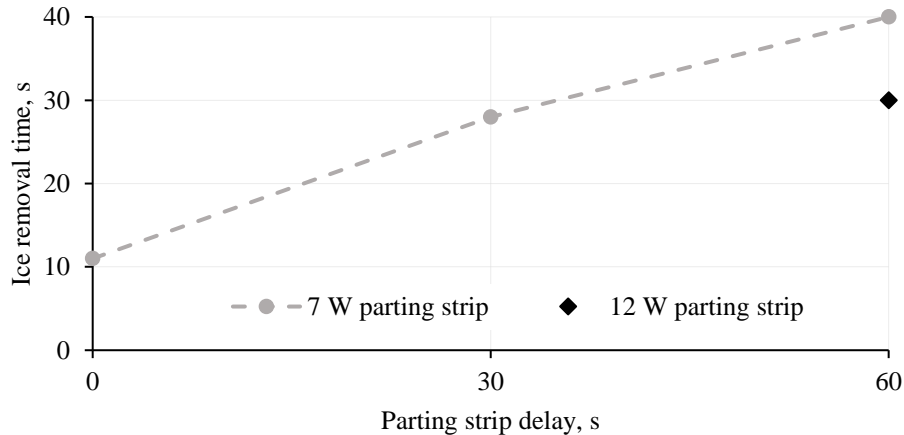


Fig. 8 The required de-icing times for different delays of parting strip activation.

IV. Discussion

The results show that higher heat fluxes lead to faster ice shedding because the ice at the ice/airfoil interface melts faster for higher heat fluxes. However, the runs with higher heat fluxes also used more energy until shedding than runs with lower heat fluxes. This effect is likely related to the heat stored in the wing and to the time the heat needs to conduct from the carbon heating zone within the wing to the surface of the wing. Hence, this could indicate that when designing a de-icing system, lower heat fluxes should be preferred over higher heat fluxes to make the IPS more energy-efficient. Lower heat fluxes could also be beneficial for the battery system since the maximum power required is lower. However, two important considerations must be made. First, if the heat flux is chosen too small, the IPS will not be able to increase the surface temperature above the melting point and the de-icing will be unsuccessful. Second, several different parameters are important for icing physics. It is difficult to measure all parameters simultaneously with good accuracy during the flight. As a result, the UAV could fly in icing conditions that require higher heat fluxes for de-icing than the conditions for which the heat flux was selected. This could lead to unsuccessful de-icing and

would require more energy due to the degraded aerodynamic performance of the iced wings. In the worst case, this could result in a crash of the aircraft. To mitigate this, the heat flux should be selected with a sufficient safety margin. The safety margin would also depend on the accuracy of sensors used in the aircraft to investigate the icing conditions. Another option for de-icing would be to switch from power-controlled de-icing to temperature-controlled de-icing. Power-controlled de-icing, as used in this study, means having constant power levels during the de-icing sequence. The heat fluxes are typically defined before the flight and take multiple ambient variables into account, for example, the ambient temperature. With temperature-controlled de-icing, the power supplied to the heating zones is controlled using a feedback loop to keep the temperature readings of one or multiple thermocouples at a defined set point. To use temperature control, the position of the thermocouples must be close to the outside of the wing and a good control algorithm is required. Hence, using a temperature controller is more complicated compared to power control. However, the temperature controller depends less on the accuracy of measurements of ambient variables since keeping the surface temperature above the freezing temperature will eventually result in de-icing for all ambient conditions.

Additionally, also the expected shedding time would have to be selected with a sufficient safety margin if shedding times are defined before the flight. This would increase the energy usage of the whole system since the zones would typically be heated longer than required to de-ice the wing. Hence, having tools that detect when ice shedding has happened could improve the energy efficiency significantly [20].

While the results of faster shedding for higher heat fluxes are in line with previous experiments [12], the energy efficiency results show differences. In the previous study, no clear trend was visible for the influence of heat fluxes on energy efficiency. This study, however, showed a clear trend of decreasing energy efficiency with increasing heat fluxes. This difference might be related to changes in the chord of the wing and the size of the zones. Additionally, the wing was manufactured slightly differently. Slight differences in the materials used and the exact build-up could play a role in the different results between the two studies considering the importance of thermal properties of the interior of the wing.

No clear indication of the effect of the secondary zone heat flux on the shedding time could be gained. Hence, more tests are necessary to check this behavior. To check if the gap between the heating zones can cause delayed shedding, more runs at cold temperatures with low secondary zone heat fluxes should be done and the surface of the wing should be monitored with a thermal-imaging camera. Since the results showed significant differences, testing at more different temperatures and with more different heat fluxes should also help to gain a better understanding of the connection between secondary zone heat fluxes and shedding times. However, the runs showed clearly that less ice sheds if the secondary zone heat flux is decreased. Hence, while it might appear to be more energy-efficient to have a low secondary zone heat flux, it must be considered that some of the ice might remain on the wing and decrease the aerodynamic performance even after the de-icing cycle. This is particularly true for runs with no heat on the secondary zone where all the ice that accreted on the unheated zones remains on the wing.

Changing the angle of attack has multiple effects on the ice shape and aerodynamics. As a result, changing the angle of attack has a significant effect on the ice shedding times. Except for two outliers, the ice shedding times showed a trend of decreasing with increasing angles of attack. This result is in line with previous experiments [12]. More tests could help to test if the outliers were due to measurement uncertainties or measurement errors, or if the shedding times increase with increasing angle of attack for some conditions. Since the shedding times were only measured for the upper side of the wing, no clear recommendation for the design or operation of an IPS can be made. As the amount of ice and the iced area both increase on the lower side for higher angles of attack, the ice shedding will likely take longer on the lower side of the aircraft for higher angles of attack. Hence, more tests are required that have a focus on ice shedding on the lower side of the wing for different angles of attack.

The results showed clearly that longer intercycle times lead to a more energy-efficient de-icing of the wing. But this finding does not necessarily mean that de-icing systems should use longer intercycle times in general. Instead, the effect the intercycle ice has on the aircraft aerodynamics must be considered as well. Longer intercycle times result in bigger ice shapes and likely also more severe ice shapes for the aircraft aerodynamics. Hence, to optimize the intercycle time of de-icing systems for energy efficiency, both, the de-icing part and the aerodynamics must be optimized. Additionally, it must be considered that the ice that sheds from the wing can hit parts downstream and damage them [21]. Thus, an analysis must be performed for the specific aircraft that checks what parts could be hit by ice shedding events and what sizes of ice those parts can withstand without damage.

One result of the autonomy of UAVs is that the UAV relies more on sensor data than manned aircraft where the pilot is an observer as well. In the case of icing that typically means that a sensor must detect icing conditions before the IPS is started. The results in this paper show that good ice detection sensors are very important for UAVs since the time until the ice is removed increases significantly for delayed parting strip activation. Even when using a parting strip design, the de-icing will be more like conventional de-icing for cases with delayed parting strip activation. Even with a good ice detection sensor, the ice detection time can vary. Hence, it is recommended to start with a de-icing

run when the sensor detects ice. It might also be better to use a larger parting strip power for this first de-icing run after ice detection since this will decrease the shedding time significantly.

In test runs with delayed activation of the parting strip, the ice typically moved laterally towards the outer side of the swept wing. This could potentially be advantageous for swept wings without winglets. Since there would be no winglets to stop the movement of the ice, the ice might just slide laterally on the wing until it sheds towards the side. However, more tests are necessary to confirm this hypothesis.

The tests had several limitations that result in uncertainties of the results. First, the IPS must be started manually. This can result in slight errors since the exact time from starting the IPS to shedding the ice is slightly uncertain. Second, a video system was in place to observe the ice shedding as well and provide further information during the post-processing of data. However, the quality of some videos is too bad to gain any knowledge. The measurement error could be reduced significantly by using an indicator that shows when the de-icing process started and by having a reliable video system that looks at the leading edge of the wing and the indicator at the same time. This would also reduce the probability of wrong measurements. Another limitation is that the heat fluxes are not measured individually but are assumed to be identical to the electric energy provided to the zones. Hence, the accuracy could be increased by measuring the heat flux at the heating zone. To provide more general results, it would be best to measure the heat flux at the surface of the wing since also the conduction between the heating zones and the wing surface depends on the exact structure of the IPS.

V. Conclusion

Atmospheric icing can limit the usability of UAVs significantly if the UAV is not equipped with a sufficient IPS. Understanding the influence of different ambient parameters and different settings on the de-icing process is important for designing an IPS. This study presented the experimental results of two wings equipped with an electrothermal IPS that were tested in an icing wind tunnel. One important result is that faster ice shedding does not always result in more energy-efficient de-icing. Instead, the results indicate that the IPS should be operated with low heat fluxes and with long intercycle times to be energy-efficient.

The study also discussed that the overall energy efficiency of a UAV in icing conditions depends on the energy efficiency of the IPS as well as the additional energy required due to the degraded aerodynamic performance of iced lifting surfaces. More research on the aerodynamic performance of iced wings is required to find the optimum intercycle time of de-icing systems. The results of this study indicate that secondary heating zones can have an impact on shedding times and especially the amount of ice that sheds but the uncertainty is too high to make definite statements. More tests should be conducted to fill the gaps in this study, especially considering different angles of attack and different heat fluxes in the secondary heating zones.

However, the existing results already provide a good basis for different areas of future work. First, the learnings of this study can be used to reduce the energy requirements of IPS and to develop more mature IPS designs. Second, the data can be compared to other models or methods. Especially comparisons with CFD methods could potentially accelerate the understanding of UAV icing and IPS for UAVs significantly. This is because using CFD methods allows for simulating many different conditions and settings in a very short time, and without the limitations in the test matrix that tests in icing wind tunnels have. Hence, verifying CFD methods with experimental results could potentially allow developing more generalized models for ice shedding on UAVs. Finally, the results can also be used to include icing and IPS in path-planning tools [22].

Acknowledgments

The work is partly sponsored by the Research Council of Norway through the Centre of Excellence funding scheme, project number 223254, AMOS, the IPN Pathplanning project with project number 318000, the IKTPLUSS project with project number 316425, and the BIA Rotors project with project number 296228.

We thank Tuomas Jokela and Mikko Tiihonen from VTT for their valuable help during the tests in the icing wind tunnel.

References

- [1] Federal Aviation Administration, “FAA Aerospace Forecast Fiscal Years 2021-2041,” Report, 2021.
- [2] Hann, R., and Johansen, T., “Unsettled Topics in Unmanned Aerial Vehicle Icing,” SAE Edge Report, 2020, doi: 10.4271/epr2020008.
- [3] Bragg, M. B., Broeren, A. P., and Blumenthal, L. A., “Iced-Airfoil Aerodynamics,” *Progress in Aerospace Sciences*, Vol. 41, No. 5, 2005, pp. 323–362, doi: 10.1016/j.paerosci.2005.07.001.
- [4] Liu, Y., Li, L., Chen, W., Tian, W., and Hu, H., “An Experimental Study on the Aerodynamic Performance Degradation

- of a UAS Propeller Model Induced by Ice Accretion Process,” *Experimental Thermal and Fluid Science*, Vol. 102, 2019, pp. 101–112, doi: 10.1016/j.expthermflusci.2018.11.008.
- [5] Cao, Y., Tan, W., and Wu, Z., “Aircraft Icing: An Ongoing Threat to Aviation Safety,” *Aerospace Science and Technology*, Vol. 75, 2018, pp. 353–385, doi: 10.1016/j.ast.2017.12.028.
- [6] Thomas, S. K., Cassoni, R. P., and MacArthur, C. D., “Aircraft Anti-Icing and de-Icing Techniques and Modeling,” *Journal of Aircraft*, Vol. 33, No. 5, 1996, pp. 841–854, doi: 10.2514/3.47027.
- [7] Hann, R., and Johansen, T. A., “UAV Icing: The Influence of Airspeed and Chord Length on Performance Degradation,” *Aircraft Engineering and Aerospace Technology*, Vol. 93, No. 5, 2021, pp. 832–841, doi: 10.1108/AEAT-06-2020-0127.
- [8] Szilder, K., and McIlwain, S., “In-Flight Icing of UAVs - The Influence of Reynolds Number on the Ice Accretion Process,” SAE Technical Paper 2011-01-2572, 2011, doi: 10.4271/2011-01-2572.
- [9] Peck, L., Ryerson, C. C., and Martel, C. J., “Army Aircraft Icing,” Cold Regions Research and Engineering Laboratory Report, 2002.
- [10] Scalea, J. R., Restaino, S., Scassero, M., Blankenship, G., Bartlett, S. T., and Wereley, N., “An Initial Investigation of Unmanned Aircraft Systems (UAS) and Real-Time Organ Status Measurement for Transporting Human Organs,” *IEEE Journal of Translational Engineering in Health and Medicine*, Vol. 6, 2018, doi: 10.1109/JTEHM.2018.2875704.
- [11] Girard, A. R., Howell, A. S., and Hedrick, J. K., “Border Patrol and Surveillance Missions Using Multiple Unmanned Air Vehicles,” *Proceedings of the IEEE Conference on Decision and Control*, No. 1, 2004, pp. 620–625.
- [12] Hann, R., Enache, A., Nielsen, M. C., Stovner, B. N., van Beeck, J., Johansen, T. A., and Borup, K. T., “Experimental Heat Loads for Electrothermal Anti-Icing and De-Icing on UAVs,” *Aerospace*, Vol. 8, No. 3, 2021, p. 83, doi: 10.3390/aerospace8030083.
- [13] HENRY, R., “Development of an Electrothermal De-Icing/Anti-Icing Model,” *30th Aerospace Sciences Meeting & Exhibit*, AIAA 92-0526, 1992.
- [14] Enache, A., Bernay, B., Glabeke, G., Planquart, P., and van Beeck, J., “Ice Shedding Phenomenon: An Experimental and Numerical Investigation,” *AIAA AVIATION 2020 FORUM*, 2020.
- [15] Tiihonen, M., Jokela, T., Makkonen, L., and Bluemink, G.-J., “VTT Icing Wind Tunnel 2.0,” *Winterwind Presentations*, 2016.
- [16] Hann, R., Borup, K., Zolich, A., Sorensen, K., Vestad, H., Steinert, M., and Johansen, T., “Experimental Investigations of an Icing Protection System for UAVs,” SAE Technical Paper 2019-01-2038, 2019, doi: 10.4271/2019-01-2038.
- [17] Hann, R., and Wallisch, J., “UAV Database,” *DataverseNo, Version 1*, 2020, doi: 10.18710/L4IIGQ.
- [18] Hansman, R. J., Breuer, K. S., Hazan, D., Reehorst, A., and Vargas, M., “Close-up Analysis of Aircraft Ice Accretion,” *31st Aerospace Sciences Meeting and Exhibit*, AIAA-93-0029, 1993.
- [19] Morris, A. S., and Langari, R., *Measurement and Instrumentation*, Elsevier, Amsterdam, Netherlands, 2012.
- [20] Løw-Hansen, B., Hann, R., and Johansen, T. A., “UAV Icing: Ice Shedding Detection Method for an Electrothermal De-Icing System,” *AIAA AVIATION 2022 FORUM (in press)*.
- [21] Papadakis, M., Yeong, H. W., and Soares, I. G., “Simulation of Ice Shedding from a Business Jet Aircraft,” *Collection of Technical Papers - 45th AIAA Aerospace Sciences Meeting*, No. 9, AIAA 2007-506, 2007.
- [22] Cheung, M., Hann, R., and Johansen, T. A., “UAV Icing: A Unified Icing Severity Index Derived from Performance Degradation,” *AIAA AVIATION 2022 FORUM (in press)*.